



INSTITUTE OF  
SPACE SCIENCE  
A subsidiary of INFNPR



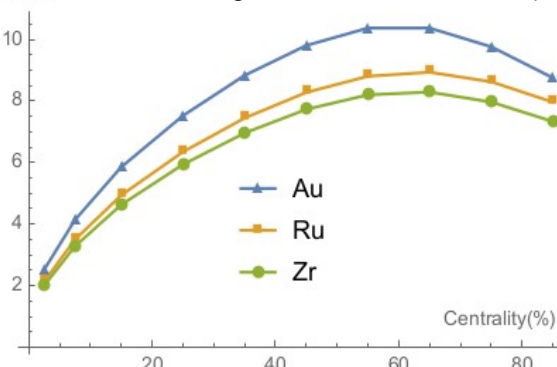
# Searches for Chiral Magnetic and Chiral Vortical Effects with ALICE

A. Dobrin for the ALICE Collaboration  
(Institute of Space Science – INFNPR Subsidiary)

The 8th International Conference on Chirality, Vorticity and Magnetic Field in Quantum Matter

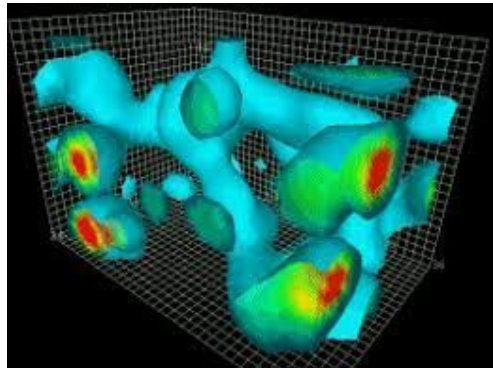
# Chiral effects in heavy-ion collisions

G-R. Liang et al., CPC 44, 094103 (2020)



Strong magnetic field  
( $B \sim 10^{15}$  T)

<http://www.physics.adelaide.edu.au/theory/staff/leinweber/VisualQCD/Nobel/>



QCD domains with P and CP  
symmetries locally broken

## Chiral Magnetic Effect (CME)

$$J_V^{\text{CME}} = \frac{\mu_A}{2\pi^2} e \vec{B}$$

**CME + CSE → Chiral Magnetic Wave (CMW)**

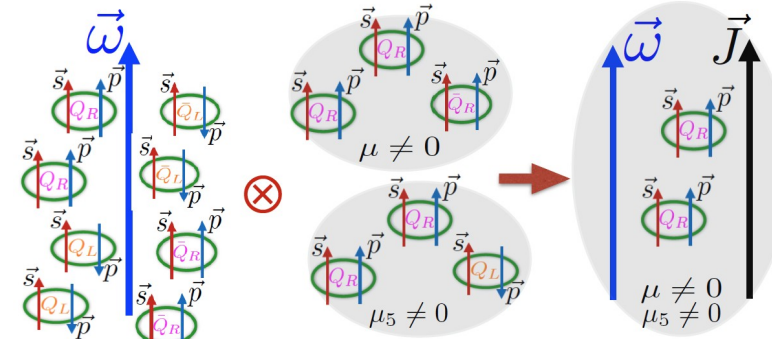
## Chiral Separation Effect (CSE)

$$J_A^{\text{CSE}} = \frac{\mu_V}{2\pi^2} e \vec{B}$$

## Chiral Vortical Effect (CVE)

$$J_V^{\text{CVE}} = \frac{\mu_V \mu_A}{\pi^2} \vec{\omega}$$

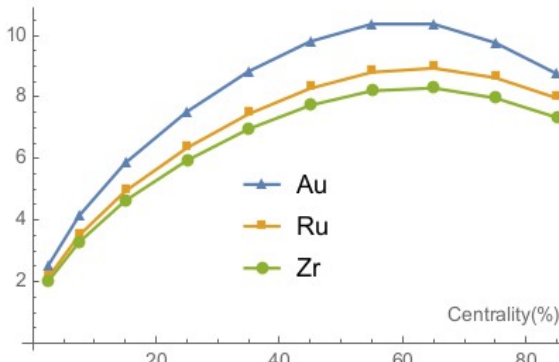
D. Kharzeev, PLB 633, 260 (2006); D. Kharzeev et al., NPA 797, 67 (2007); D. Son et al., PRL 103, 191601 (2009); Y. Burnier et al., PRL 107, 052303 (2011); D. Kharzeev, PRL 106, 062301 (2011); D. Kharzeev et al., PRD 83, 085007 (2011); D. Kharzeev et al, PPNP 88, 1 (2016)



Electric current along the magnetic  
field → charge separation

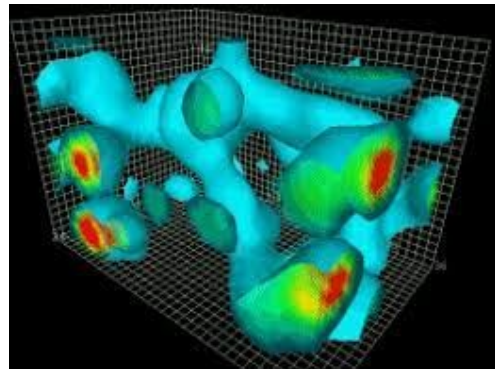
# Chiral effects in heavy-ion collisions

G-R. Liang et al., CPC 44, 094103 (2020)

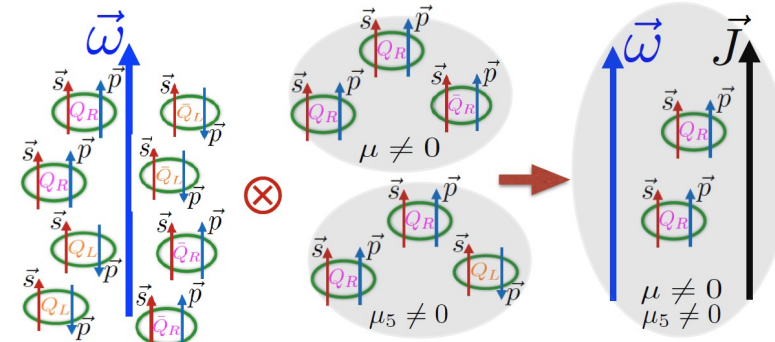


Strong magnetic field  
( $B \sim 10^{15}$  T)

<http://www.physics.adelaide.edu.au/theory/staff/leinweber/VisualQCD/Nobel/>



QCD domains with P and CP  
symmetries locally broken



Electric current along the magnetic  
field  $\rightarrow$  charge separation

## Chiral Magnetic Effect (CME)

$$J_V^{\text{CME}} = \frac{\mu_A}{2\pi^2} e \vec{B}$$

CME + CSE  $\rightarrow$  Chiral Magnetic Wave (CMW)

## Chiral Separation Effect (CSE)

$$J_A^{\text{CSE}} = \frac{\mu_V}{2\pi^2} e \vec{B}$$

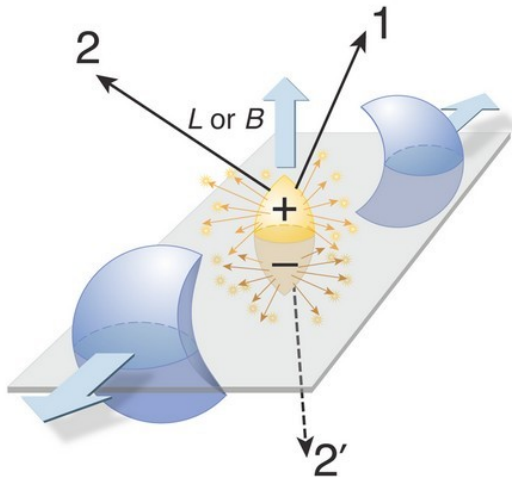
## Chiral Vortical Effect (CVE)

$$J_V^{\text{CVE}} = \frac{\mu_V \mu_A}{\pi^2} \vec{\omega}$$

D. Kharzeev, PLB 633, 260 (2006); D. Kharzeev et al., NPA 797, 67 (2007); D. Son et al., PRL 103, 191601 (2009); Y. Burnier et al., PRL 107, 052303 (2011); D. Kharzeev, PRL 106, 062301 (2011); D. Kharzeev et al., PRD 83, 085007 (2011); D. Kharzeev et al, PPNP 88, 1 (2016)

Interpretation of the results complicated by background contributions

# Observables



## CME / CVE

$$\frac{dN}{d\Delta\varphi_\alpha} \sim 1 + 2v_{1,\alpha} \cos(\Delta\varphi_\alpha) + 2a_{1,\alpha} \sin(\Delta\varphi_\alpha) + 2v_{2,\alpha} \cos(2\Delta\varphi_\alpha) + \dots,$$

### 2-particle correlator

$$\delta_m = \langle \cos[m(\varphi_a - \varphi_b)] \rangle$$

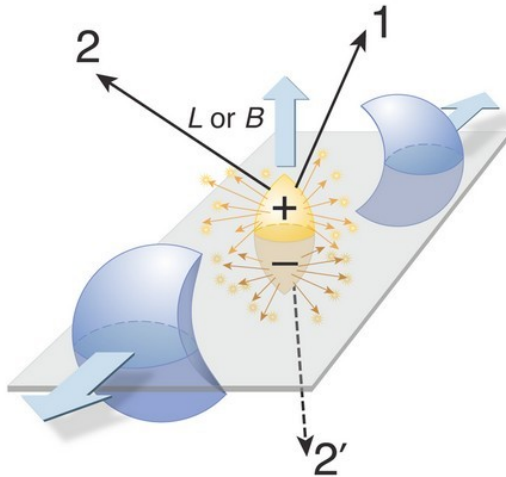
STAR, PRC 81, 054908 (2009)

### 3-particle correlator

$$\gamma_{m,n} = \langle \cos(m\varphi_a + n\varphi_b - (m+n)\Psi_{|m+n|}) \rangle$$

S. Voloshin, PRC 70, 057901 (2004)

# Observables



2-particle correlator

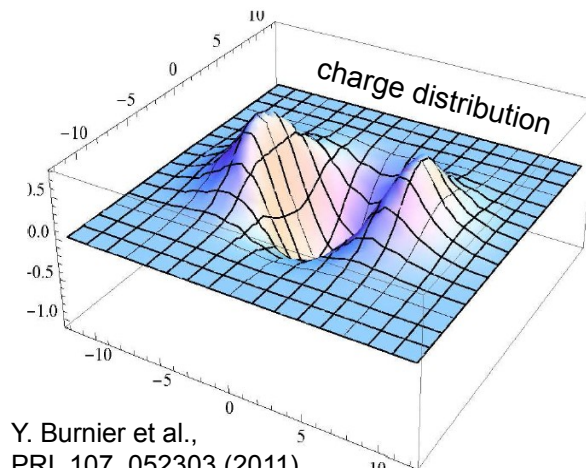
$$\delta_m = \langle \cos[m(\varphi_a - \varphi_b)] \rangle$$

STAR, PRC 81, 054908 (2009)

3-particle correlator

$$\gamma_{m,n} = \langle \cos(m\varphi_a + n\varphi_b - (m+n)\Psi_{|m+n|}) \rangle$$

S. Voloshin, PRC 70, 057901 (2004)



**CME / CVE**

$$\frac{dN}{d\Delta\varphi_\alpha} \sim 1 + 2v_{1,\alpha} \cos(\Delta\varphi_\alpha) + 2a_{1,\alpha} \sin(\Delta\varphi_\alpha) + 2v_{2,\alpha} \cos(2\Delta\varphi_\alpha) + \dots,$$

**CMW**

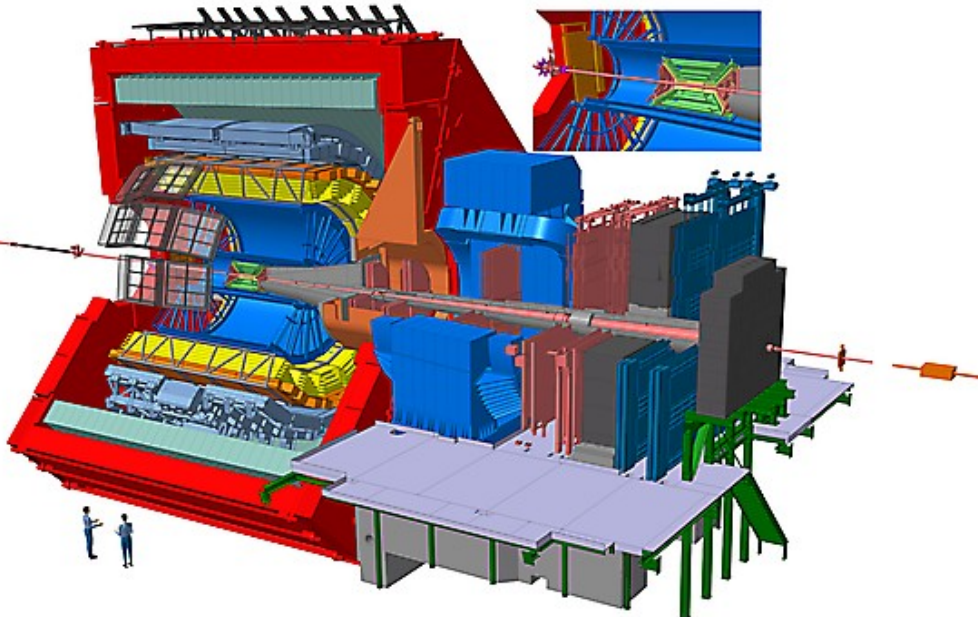
Normalized slope  $r_n^{\text{Norm}}$   
of anisotropic flow difference vs. charge asymmetry

$$\Delta v_n^{\text{Norm}} = \frac{v_n^- - v_n^+}{(v_n^- + v_n^+)/2} \propto r_n^{\text{Norm}} A \quad A = \frac{N^+ - N^-}{N^+ + N^-}$$

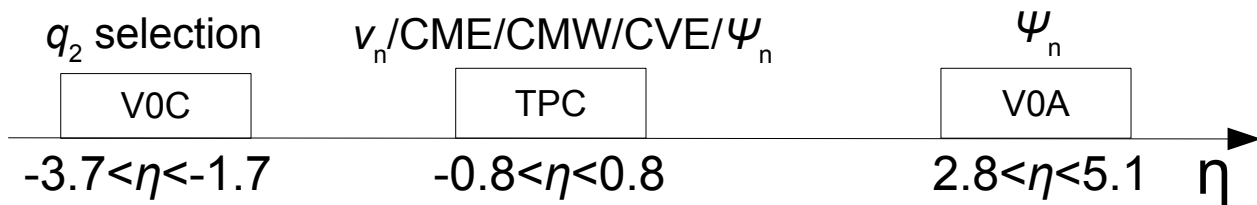
Integral covariance  $\Delta \text{IC} = \langle v_n^\pm A \rangle - \langle v_n^\pm \rangle \langle A \rangle$

S. Voloshin and R. Belmont, NPA 931, 992 (2014)

# A Large Ion Collider Experiment



- Inner Tracking System (ITS)
  - Tracking, vertexing
- Time Projection Chamber (TPC)
  - Tracking, vertexing, particle identification based on specific energy loss,  $\Psi_n$
- Time-of-Flight (TOF)
  - Particle identification based on flight time
- V0 detector
  - Triggering, centrality,  $\Psi_n$
- Track selection
  - $0.2 < p_T < 5 \text{ GeV}/c, |\eta| < 0.8$

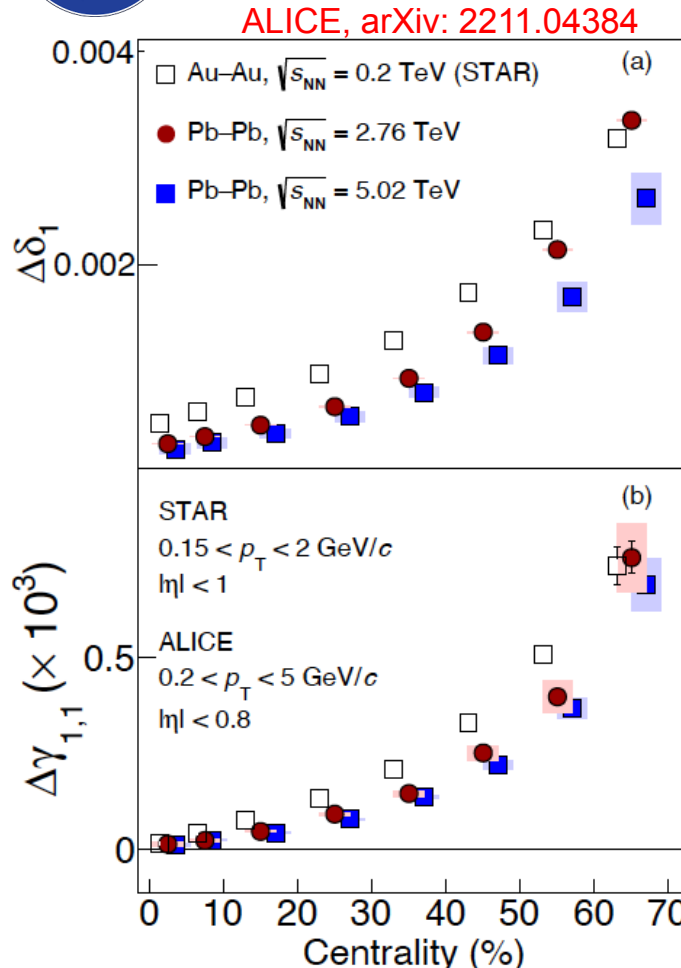


- Pb–Pb at  $\sqrt{s_{\text{NN}}} = 5.02 \text{ TeV}$ 
  - $\sim 235M$  events
- Xe–Xe at  $\sqrt{s_{\text{NN}}} = 5.44 \text{ TeV}$ 
  - $\sim 1M$  events



# Chiral Magnetic Effect

## CME @ LHC



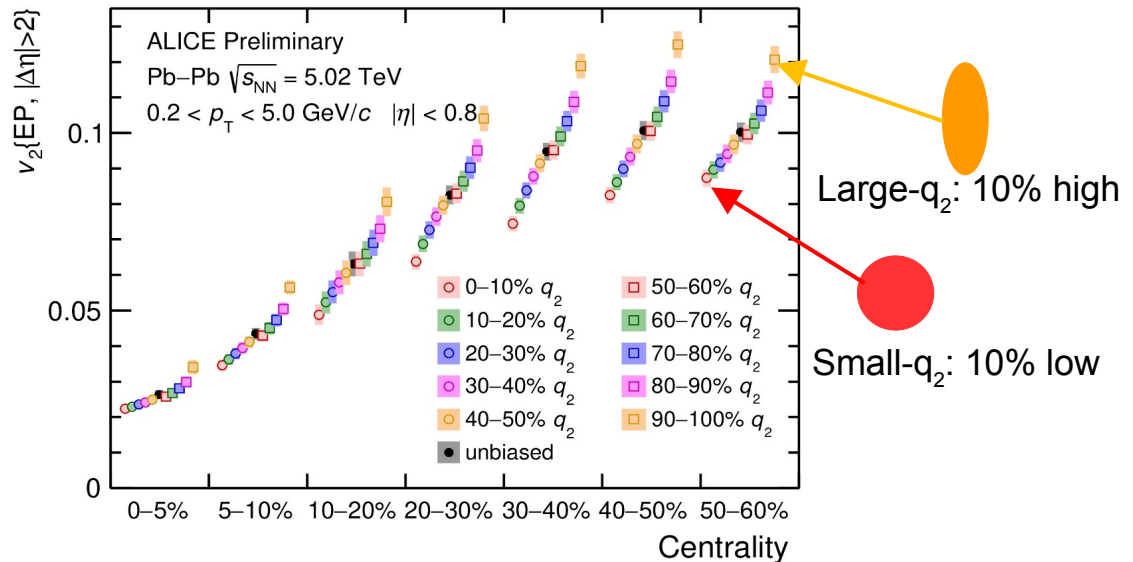
- Strong centrality dependence consistent with naive expectations from CME
- Similar magnitude between RHIC and LHC
  - Different dilution effects (3x larger  $dN_{ch}/d\eta$  at LHC than at RHIC)
  - Different magnitude of the magnetic field
- Large contribution from background → local charge conservation (LCC) coupled with anisotropic flow
  - Various approaches used to disentangle signal from background
    - Vary the background ( $v_2$ ) → event shape engineering
    - “Killing” the signal (B) → higher harmonics
    - Vary the signal (B) → different collision systems

S. Schlichting and S. Pratt, PRC 83, 014913 (2011)



# Varying the background using event shape engineering

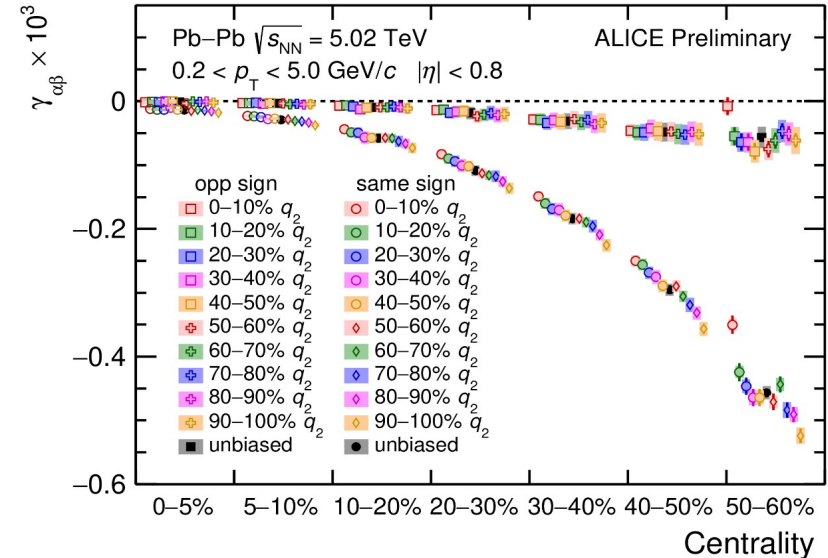
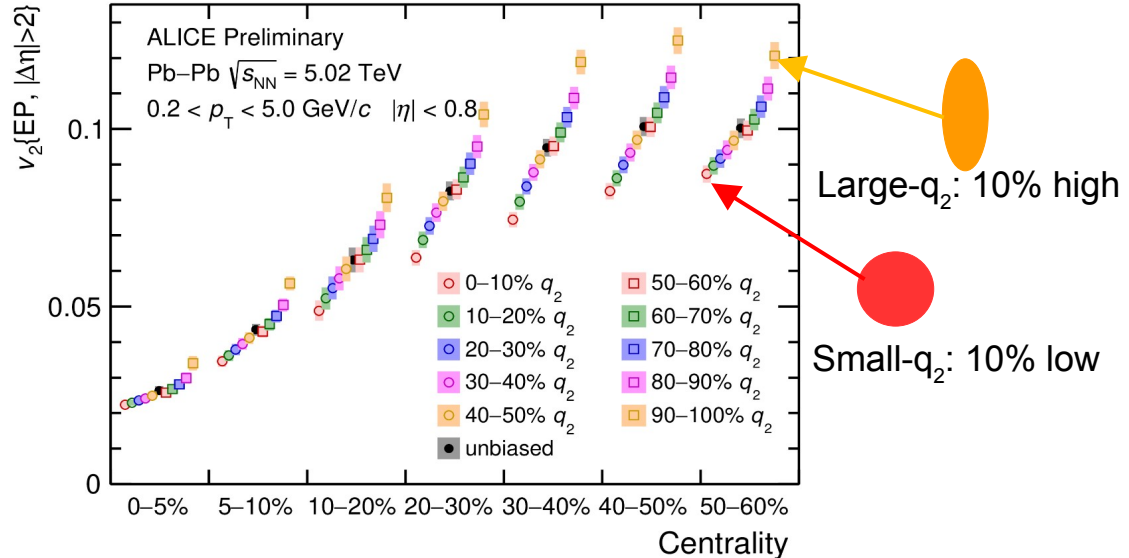
## CME with ESE (I)



ALI-PREL-550463

- $q_2^{\text{VOC}}$  used to select events with 30% larger or 25% smaller  $v_2$  than the average

# CME with ESE (I)

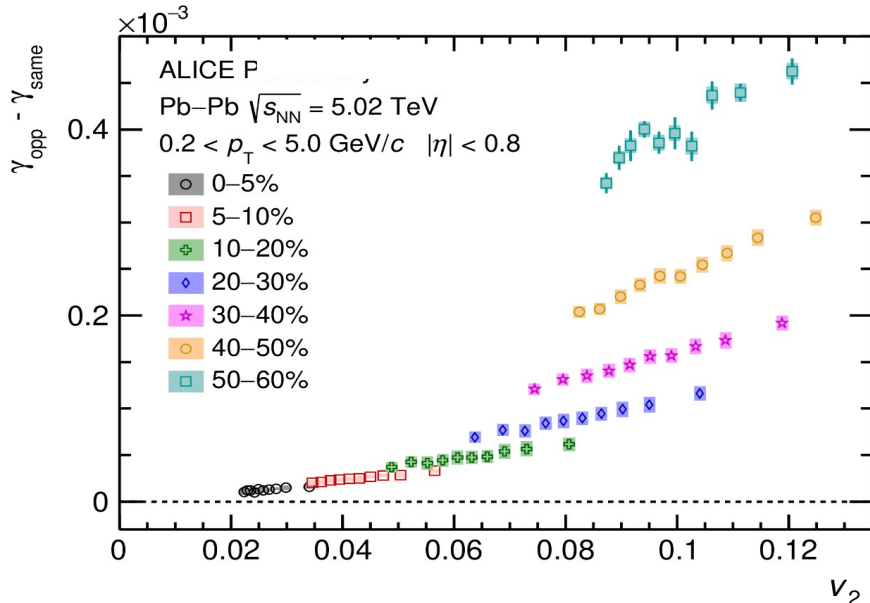


ALI-PREL-550463

ALI-PREL-550472

- $q_2^{\text{VOC}}$  used to select events with 30% larger or 25% smaller  $v_2$  than the average
- $\gamma_{\alpha\beta}$  contains potential CME signal as well as background effects
  - Background contributions are suppressed at the level of  $v_2$
- $\gamma_{\alpha\beta}$  depends on the event shape selection in a given centrality bin

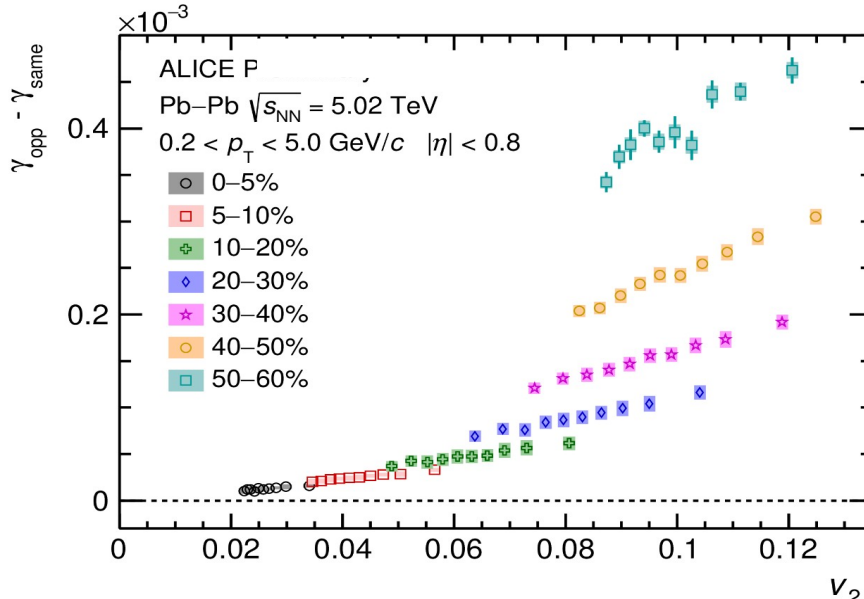
## CME with ESE (II)



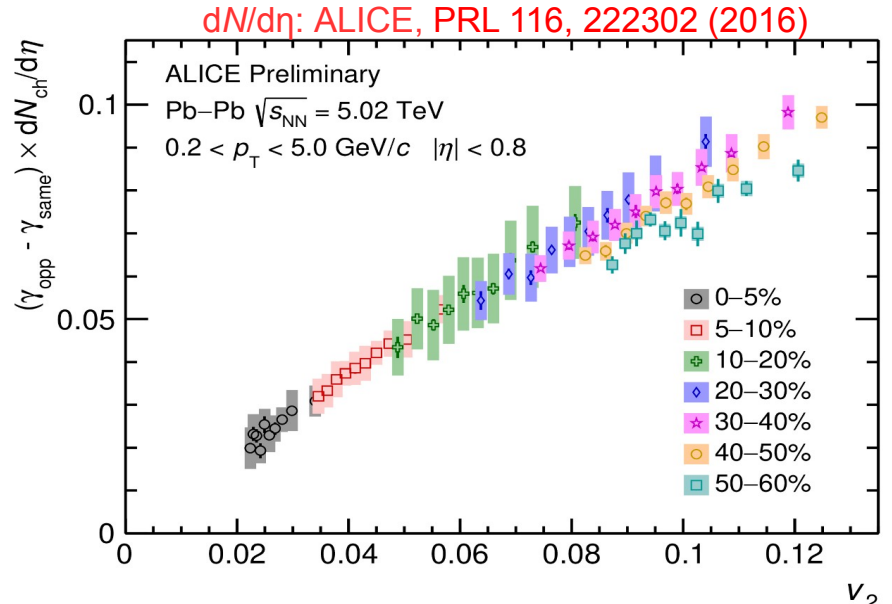
ALI-PREL-550475

- $\gamma_{ab}$  (opp-same) can be used to study the CME
  - Difference is positive for all centrality classes and decreases with centrality and  $v_2$  (in a given centrality bin)

# CME with ESE (II)



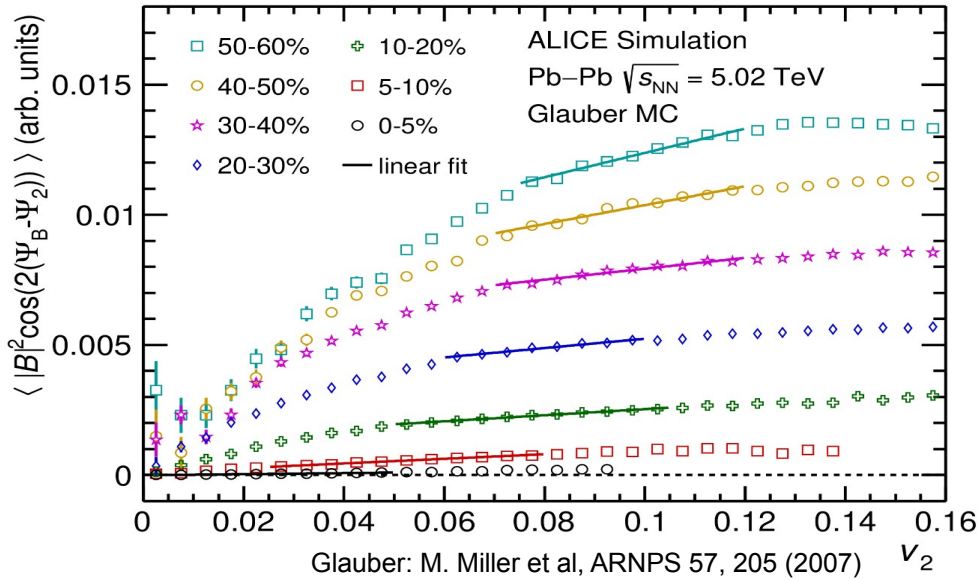
ALI-PREL-550475



ALI-PREL-550481

- $\gamma_{ab}$  (opp-same) can be used to study the CME
  - Difference is positive for all centrality classes and decreases with centrality and  $v_2$  (in a given centrality bin)
  - Difference approximately scales with  $v_2$  and multiplicity → mostly background contribution

# Does magnetic field depend on $v_2$ in initial state models?



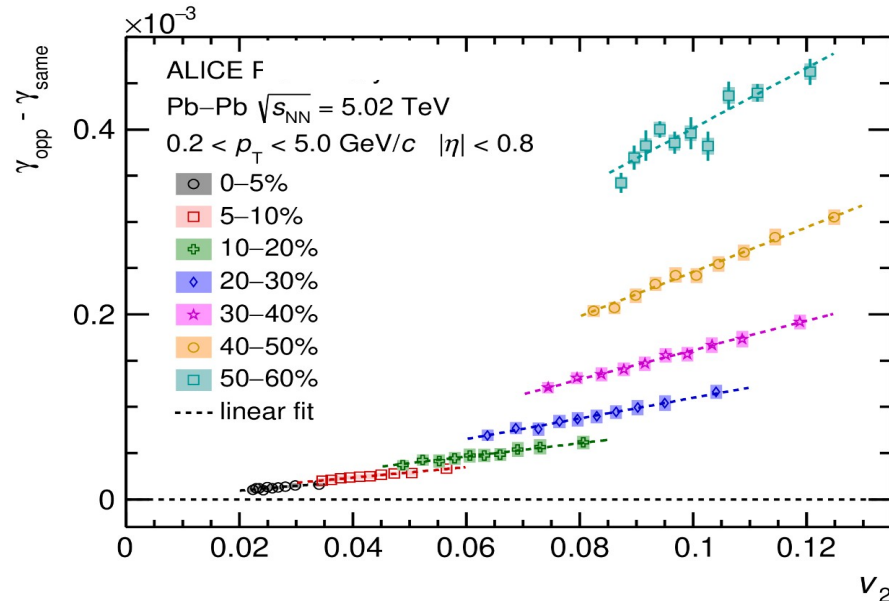
$$eB_s^\pm(\tau, \eta, \mathbf{x}_\perp) = \pm Z\alpha_{EM} \sinh(Y_0 \mp \eta) \int d^2x'_\perp \rho_\pm(x'_\perp) [1 - \theta_\mp(x'_\perp)] \times \frac{(x'_\perp - \mathbf{x}_\perp) \times \mathbf{e}_z}{[(x'_\perp - \mathbf{x}_\perp)^2 + \tau^2 \sinh(Y_0 \mp \eta)^2]^{3/2}}$$

D. Kharzeev et al., NPA 803, 227 (2008)

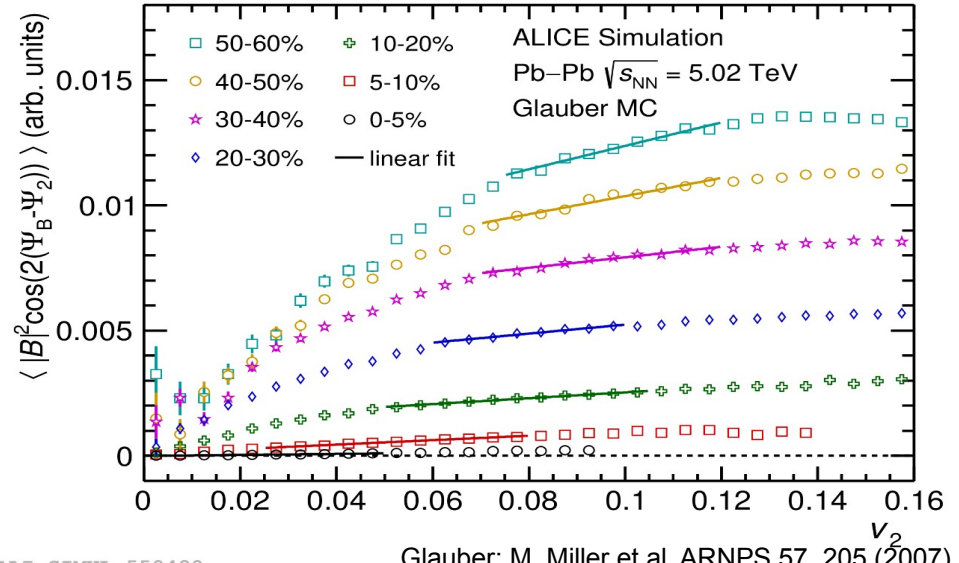
ALI-SIMUL-550490

- Perform a MC Glauber simulation to evaluate the dependence of the CME signal on  $v_2$ 
  - Parameters are tuned to ALICE results
  - Calculate magnetic field at the origin using spectators with the proper time  $\tau=0.1 \text{ fm}$
  - $\langle |B|^2 \cos(2(\Psi_B - \Psi_2)) \rangle$ , the expected contribution of the CME to  $\gamma_{ab}$ , shows a strong dependence on  $v_2$

# Relating data and models



ALI-PREL-550478



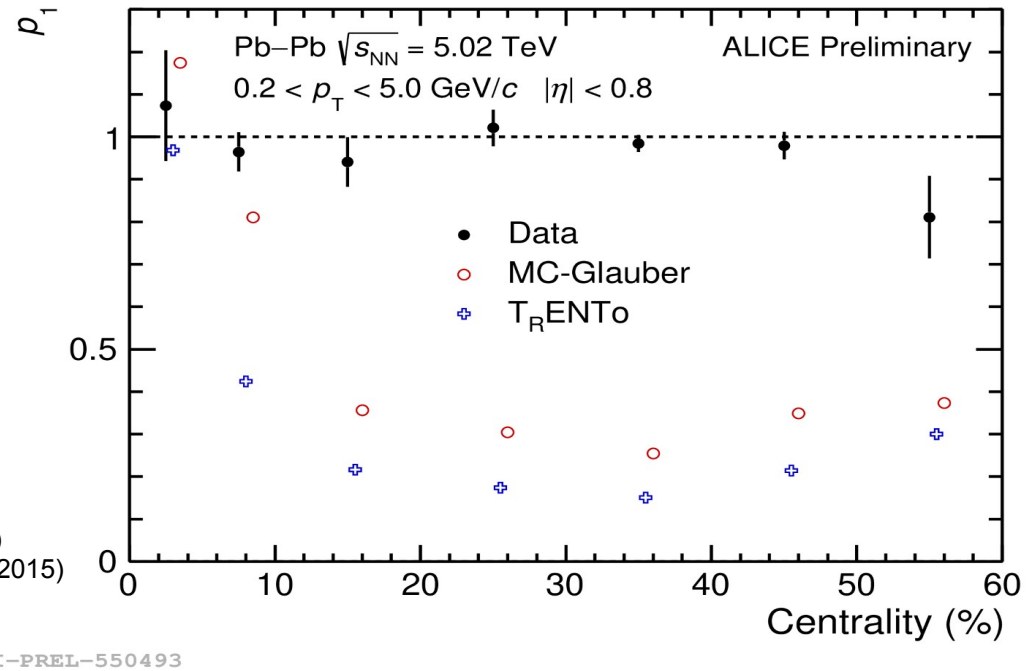
ALI-SIMUL-550490

Glauber: M. Miller et al, ARNPS 57, 205 (2007)

- Fit  $\gamma_{ab}$  (opp-same) and  $\langle |B|^2 \cos(2(\Psi_B - \Psi_2)) \rangle$  with a linear function to disentangle the potential CME signal from background

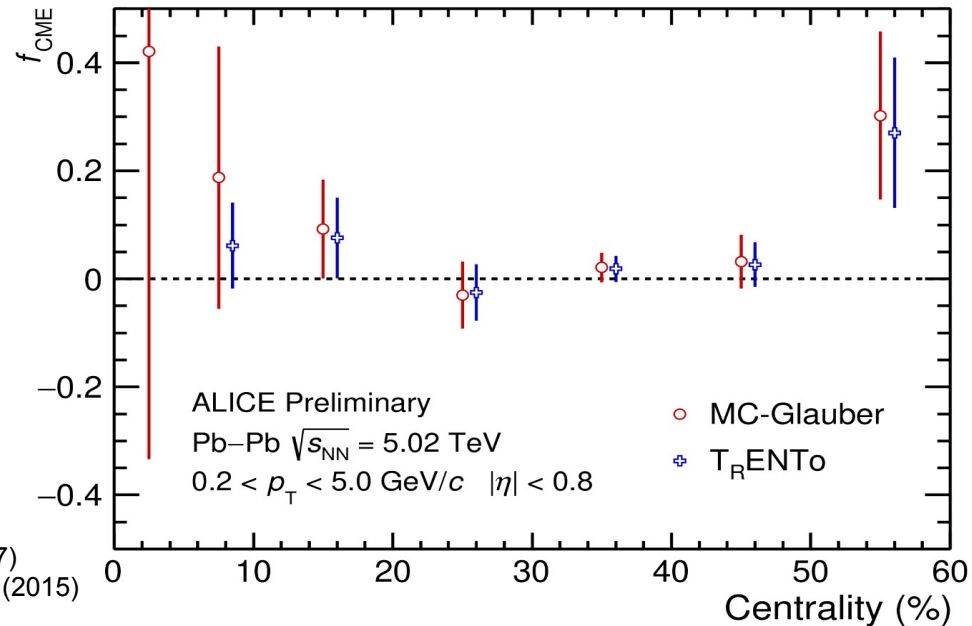
$$P_1(v_2) = p_0(1 + p_1(v_2 - \langle v_2 \rangle)/\langle v_2 \rangle)$$

# Slopes of data and model fits



- Extract the CME fraction,  $f_{\text{CME}}$  relating the slopes of data and model fits according to
$$f_{\text{CME}} * p_{1, \text{MC}} + (1 - f_{\text{CME}}) * 1 = p_{1, \text{data}}$$
- Assumption: background contribution scales linearly with  $v_2$  and the corresponding slope is unity

## CME fraction



Glauber: M. Miller et al, ARNPS 57, 205 (2007)

TRENTO: J. Moreland et al, PRC 92, 011901 (2015)

ALI-PREL-550496

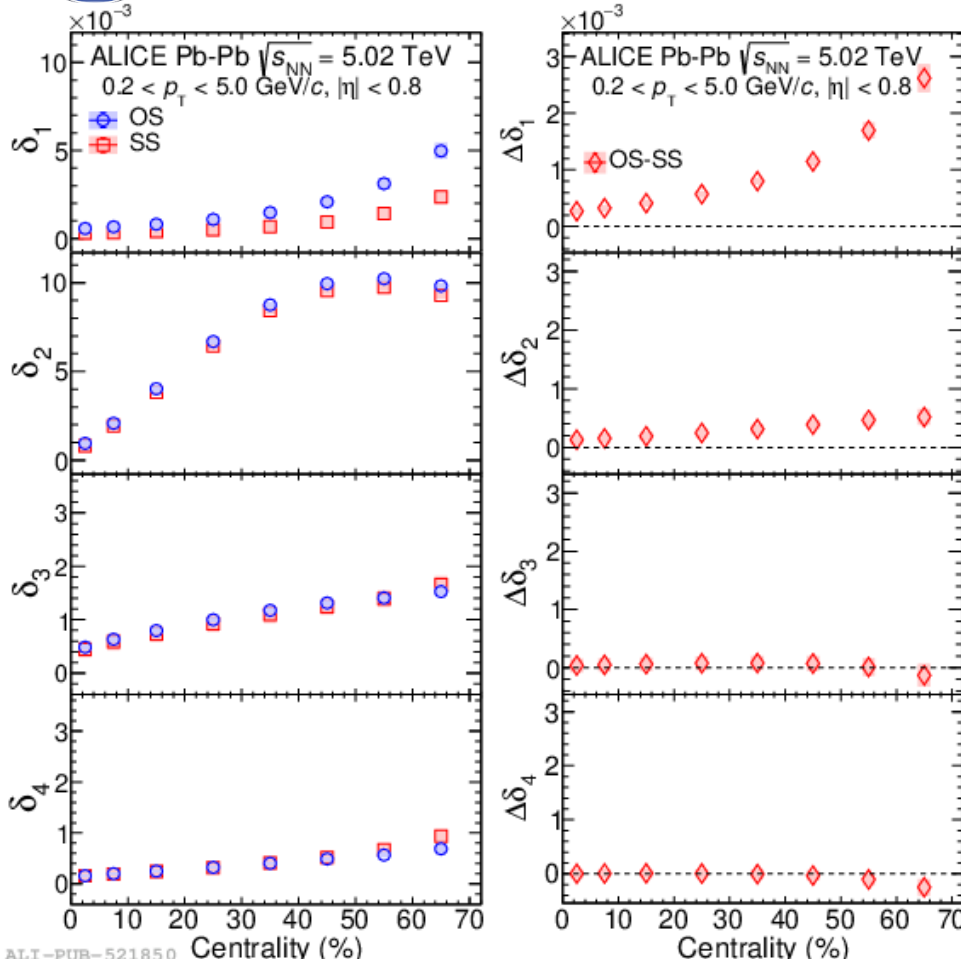
- CME fraction in 0–5% is currently statistically limited
- Combining the points from 5–60% gives
  - $f_{\text{CME}}(\text{Glauber}) = 0.028 \pm 0.021 \rightarrow 6.4\% \text{ at 95\% C.L.}$
  - $f_{\text{CME}}(\text{T}_R\text{ENTo}) = 0.025 \pm 0.018 \rightarrow 5.5\% \text{ at 95\% C.L.}$



# “Killing” the signal using higher harmonics

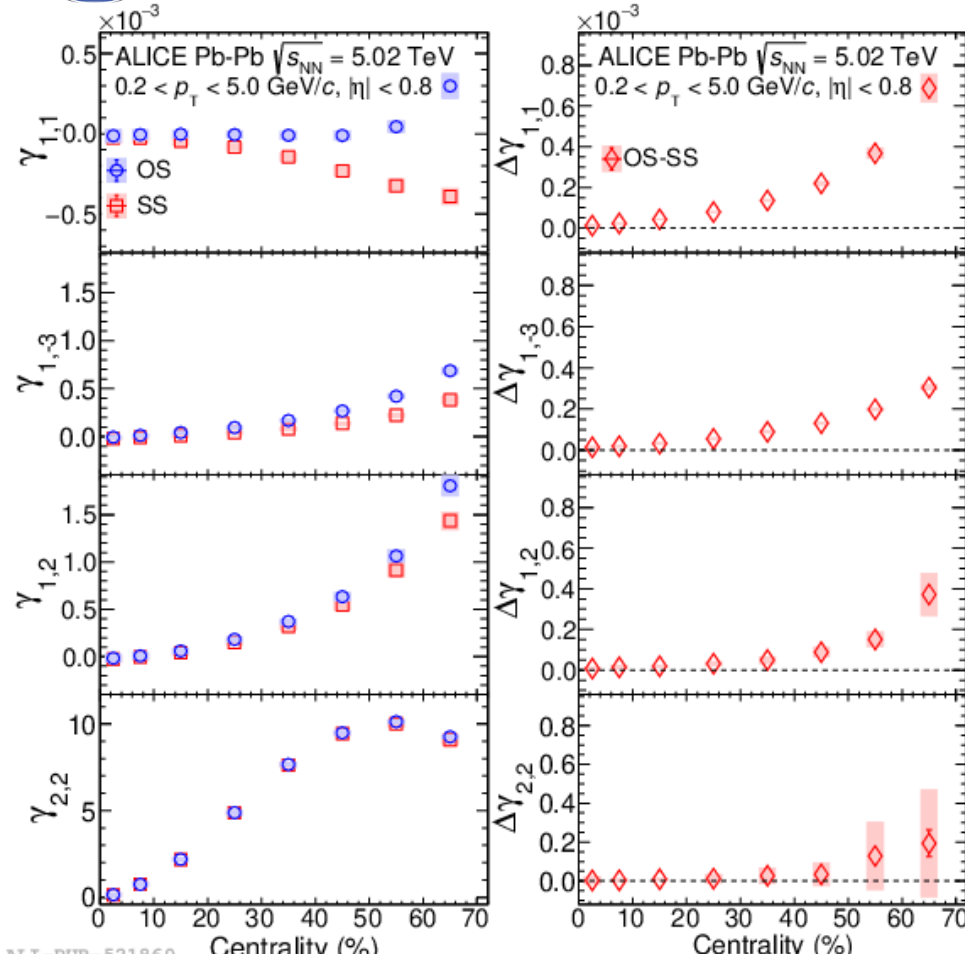
ALICE, JHEP 09, 160 (2020)

# 2-particle correlators



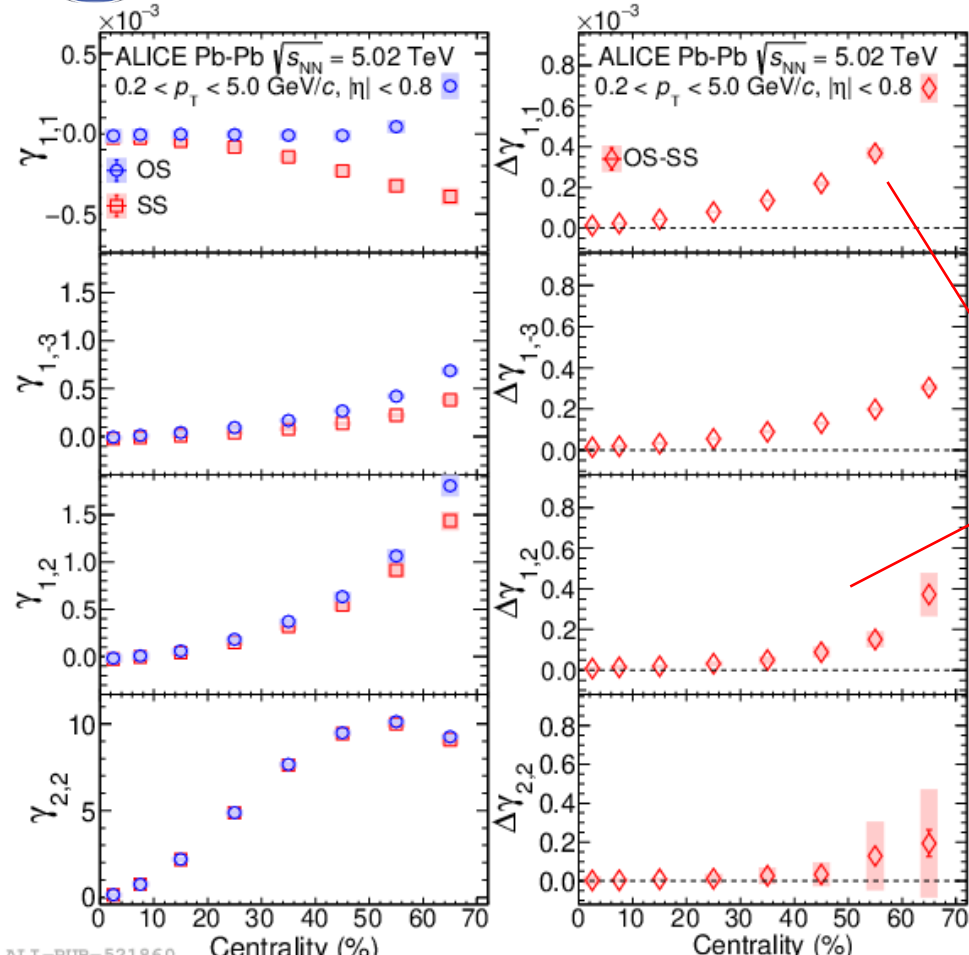
- Weak charge dependence, except  $\delta_1$ 
  - Dominated by background effects → constrain background in  $\gamma_{1,1}$

# 3-particle correlators



- $\gamma_{1,1}$  and  $\gamma_{1,3}$  sensitive to CME
- $\gamma_{1,2}$  and  $\gamma_{2,2}$  probe only the background
- Significant charge dependence, except  $\gamma_{2,2}$ 
  - Increases from central to peripheral collisions

# 3-particle correlators



- $\gamma_{1,1}$  and  $\gamma_{1,3}$  sensitive to CME
- $\gamma_{1,2}$  and  $\gamma_{2,2}$  probe only the background
- Significant charge dependence, except  $\gamma_{2,2}$ 
  - Increases from central to peripheral collisions
- $\gamma_{1,1}$  and  $\gamma_{1,2}$  used to estimate the background contribution to  $\gamma_{1,1}$

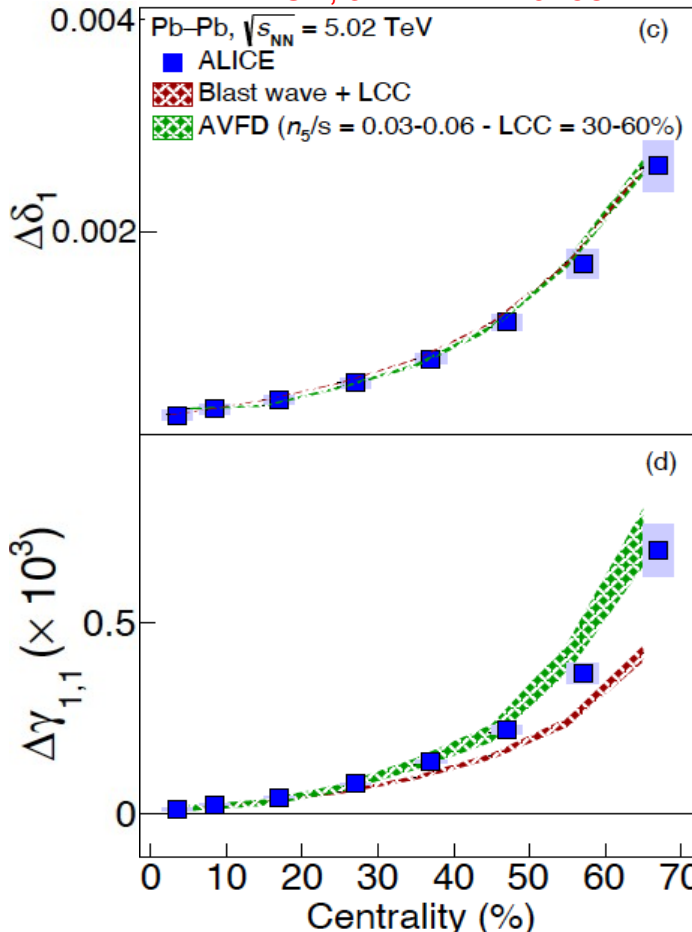
$$\Delta\gamma_{1,1} \approx \kappa_2 v_2 \Delta\delta_1$$

$$\Delta\gamma_{1,2} \approx \kappa_3 v_3 \Delta\delta_1 \longrightarrow \Delta\gamma_{1,1}^{\text{Bkg}} \approx \Delta\gamma_{1,2} \times \frac{v_2}{v_3} \frac{\kappa_2}{\kappa_3}$$

$$\Delta\gamma_{2,2} \approx \kappa_4 v_4 \Delta\delta_2$$

# Model comparisons

ALICE, arXiv: 2211.04384



- Blast-Wave + Local Charge Conservation (LCC)
  - Tune the parameters in each centrality class to reproduce  $v_2$  and  $p_T$  spectra of  $\pi$ ,  $K$ ,  $p$
  - Tune the number of sources emitting balancing pairs
  - Underestimates  $\Delta\gamma_{1,1}$  by up to  $\approx 40\%$ 
    - Disagreement increases from central to peripheral collisions

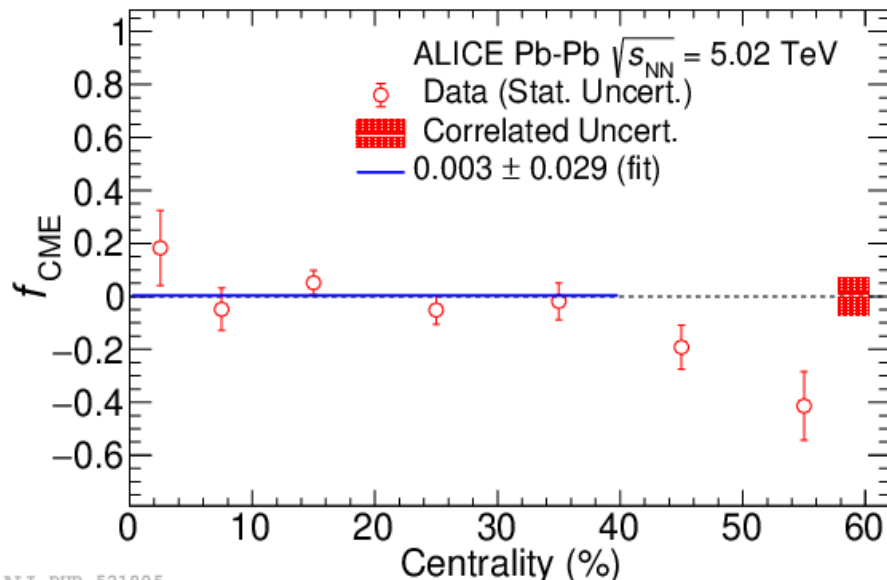
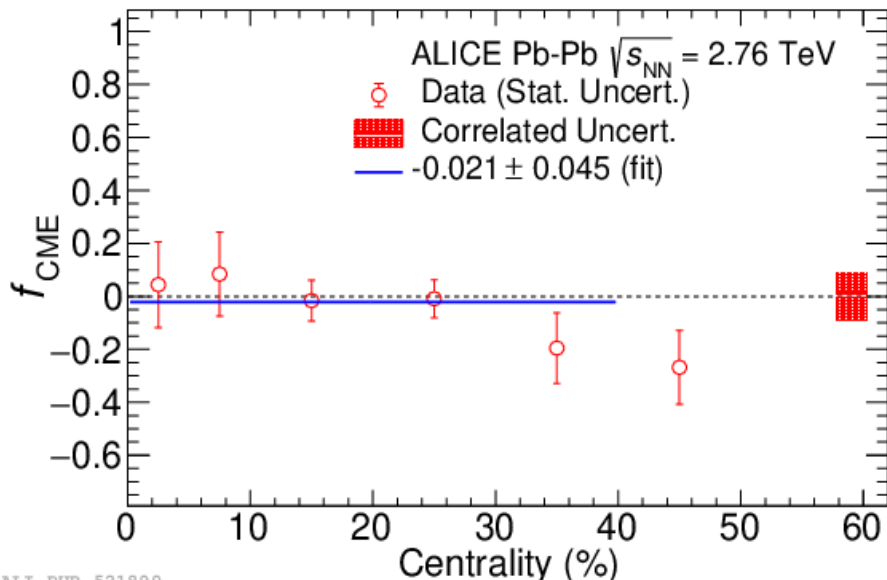
- Anomalous Viscous Fluid Dynamics (AVFD)
  - EbyE IC + E/M fields (field lifetime as input)
  - Tune the parameters in each centrality class to reproduce  $v_2$  and multiplicity
  - Good agreement with data points
    - Non-zero values for signal

P. Christakoglou et al., EPJC 81, 717 (2021)

S. Shi et al., AP 394, 50 (2018)

Y. Jiang et al., CPC 42, 011001 (2018)

# CME fraction



- Consistent with 0 for 0–40% and then becomes negative
- Combining the points from 0–40%
  - $f_{\text{CME}}^{2.76 \text{ TeV}} = -0.021 \pm 0.045 \rightarrow 18\% \text{ at 95\% C.L.}$
  - $f_{\text{CME}}^{5.02 \text{ TeV}} = 0.003 \pm 0.029 \rightarrow 15\% \text{ at 95\% C.L.}$

$$f_{\text{CME}} = 1 - \frac{\Delta\gamma_{1,1}^{\text{Bkg}}}{\Delta\gamma_{1,1}}$$

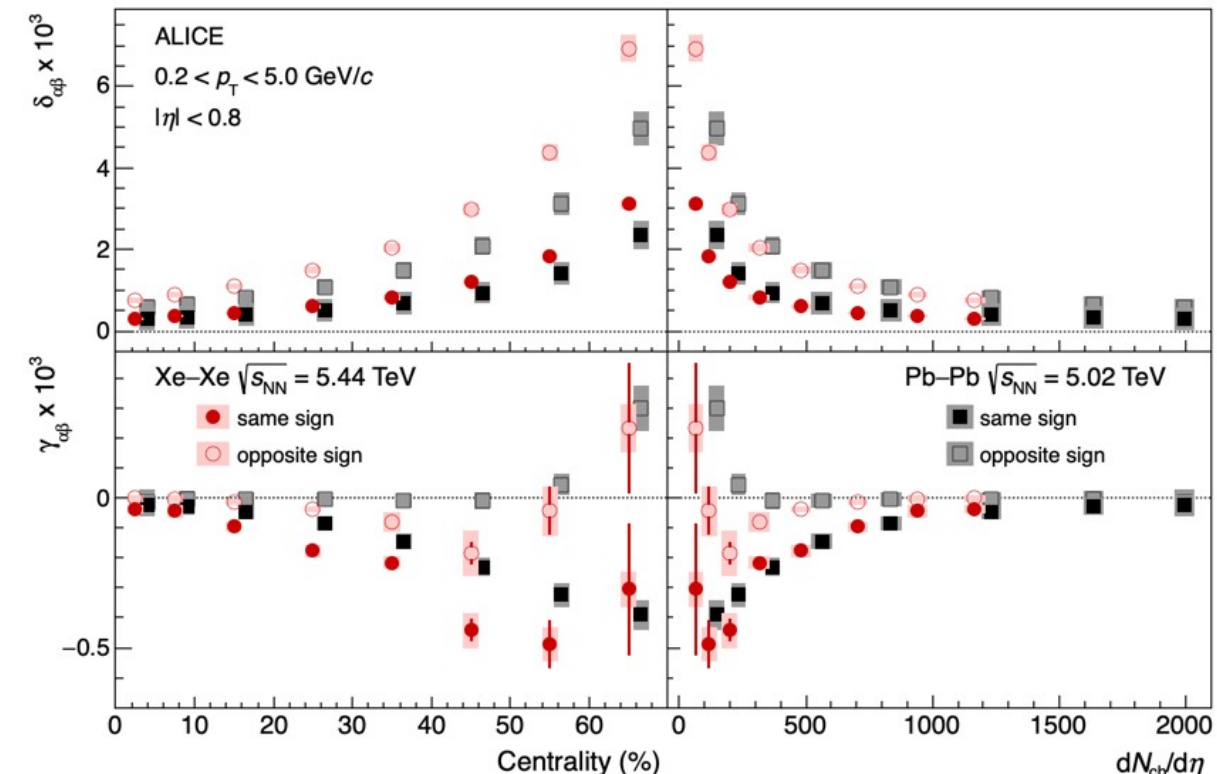
Assumption:  $K_2 \approx K_3$



# Varying the signal using different collision systems: Xe–Xe vs Pb–Pb collisions

ALICE, PLB 856, 138862 (2024)

# CME in Xe–Xe and Pb–Pb collisions

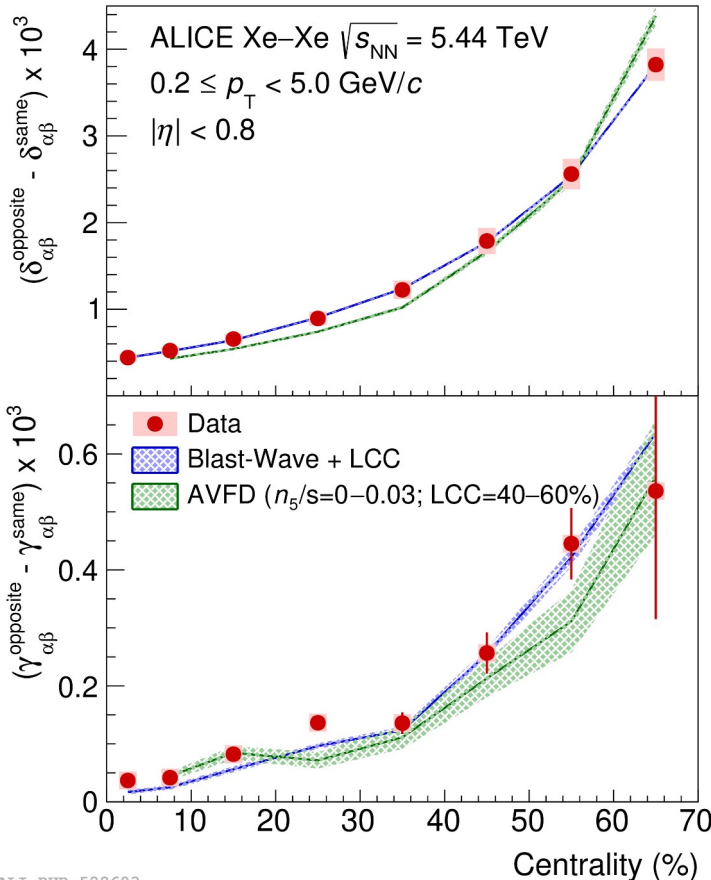


- Strong dependence on the charge
- Qualitatively similar centrality dependence
  - Larger magnitude in Xe–Xe than in Pb–Pb collisions
    - Dilution effects arising from different number of particles (CME  $\sim 1/M$ )
- Similar values in Xe–Xe and Pb–Pb collisions within uncertainties (vs  $dN_{ch}/d\eta$ )

ALICE, JHEP 09, 160 (2020)

ALICE, PRL 116, 222302 (2016)  
 ALICE, PLB 790, 35 (2019)

# Model comparisons



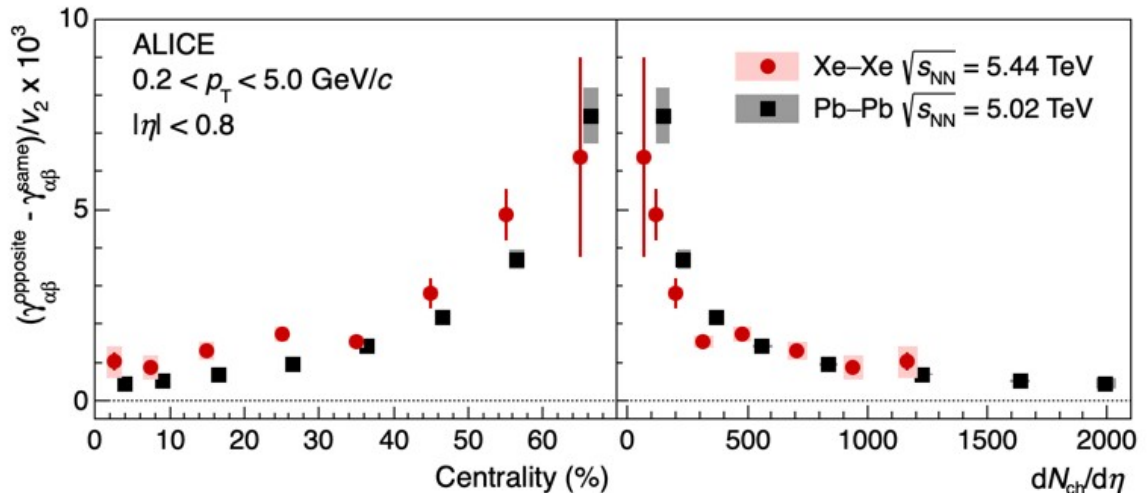
- Blast-Wave + Local Charge Conservation (LCC)
  - Describes fairly well the measured data points
    - Background dominates measurements
    - Not observed in Pb-Pb collisions
- Anomalous Viscous Fluid Dynamics (AVFD)
  - Good agreement with data points
    - Signal consistent with zero

P. Christakoglou et al., EPJC 81, 717 (2021)

S. Shi et al., AP 394, 50 (2018)

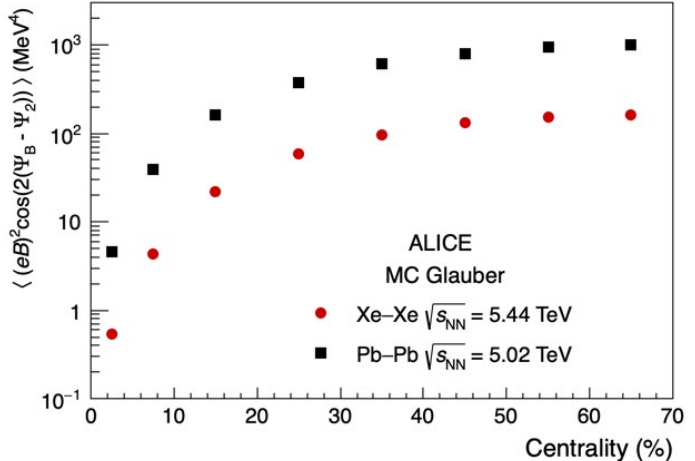
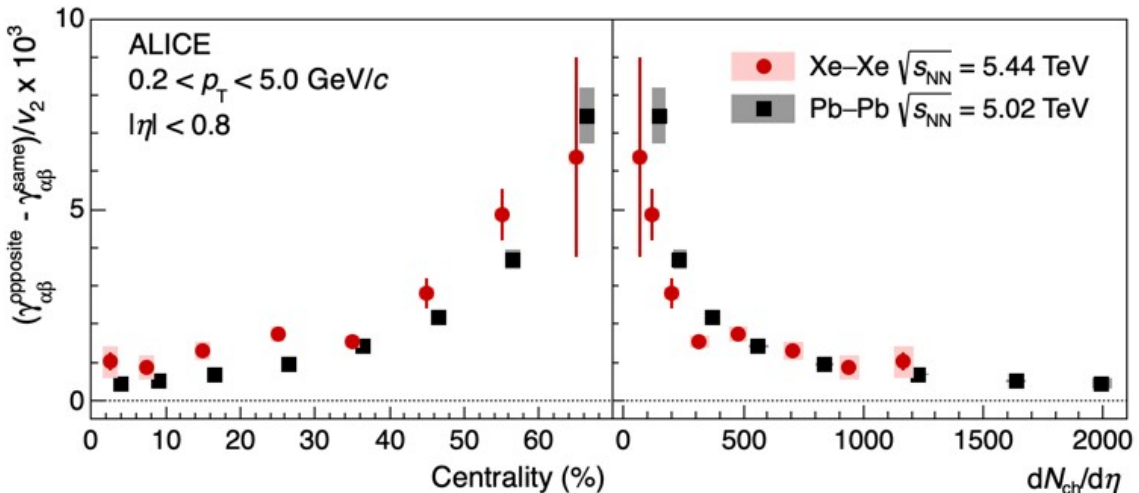
Y. Jiang et al., CPC 42, 011001 (2018)

# CME fraction in Xe–Xe and Pb–Pb collisions



- $\gamma_{ab}$  (opp-same) can be used to study CME
  - Similar values in Xe–Xe and Pb–Pb collisions (vs  $dN_{ch}/d\eta$ ) → large background contribution

# CME fraction in Xe–Xe and Pb–Pb collisions

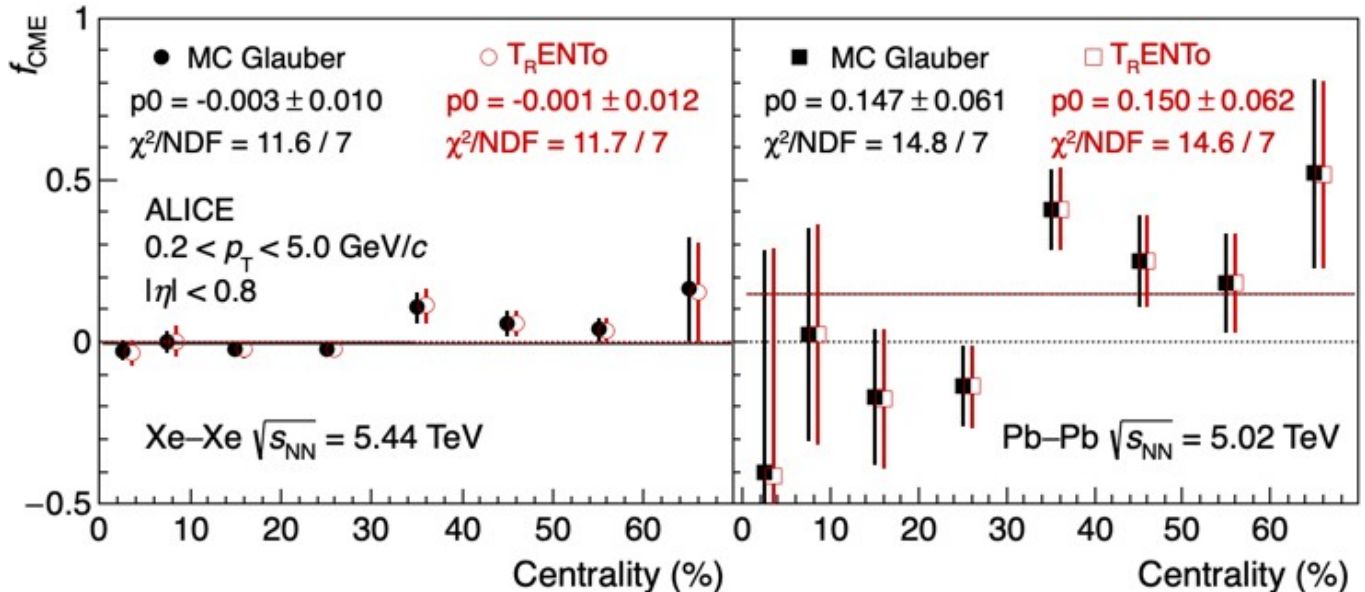


- $\gamma_{ab}$  (opp-same) can be used to study CME
  - Similar values in Xe–Xe and Pb–Pb collisions (vs  $dN_{ch}/d\eta$ ) → large background contribution
- CME fraction extracted using a two-component approach
  - Assumption: both signal and background scale with  $dN_{ch}/d\eta$ 
    - $dN_{ch}/d\eta$  used to compensate for dilution
  - $\langle |B|^2 \cos(2(\Psi_B - \Psi_2)) \rangle$  from MC simulations

$$\begin{aligned} (\frac{d N_{ch}}{d \eta})^{Xe} \Delta \gamma_{ab}^{Xe} &= s B^{Xe} + b v_2^{Xe} \\ (\frac{d N_{ch}}{d \eta})^{Pb} \Delta \gamma_{ab}^{Pb} &= s B^{Pb} + b v_2^{Pb} \end{aligned}$$

$$f_{CME} = \frac{s B}{s B + b v_2}$$

# CME fraction in Xe–Xe and Pb–Pb collisions



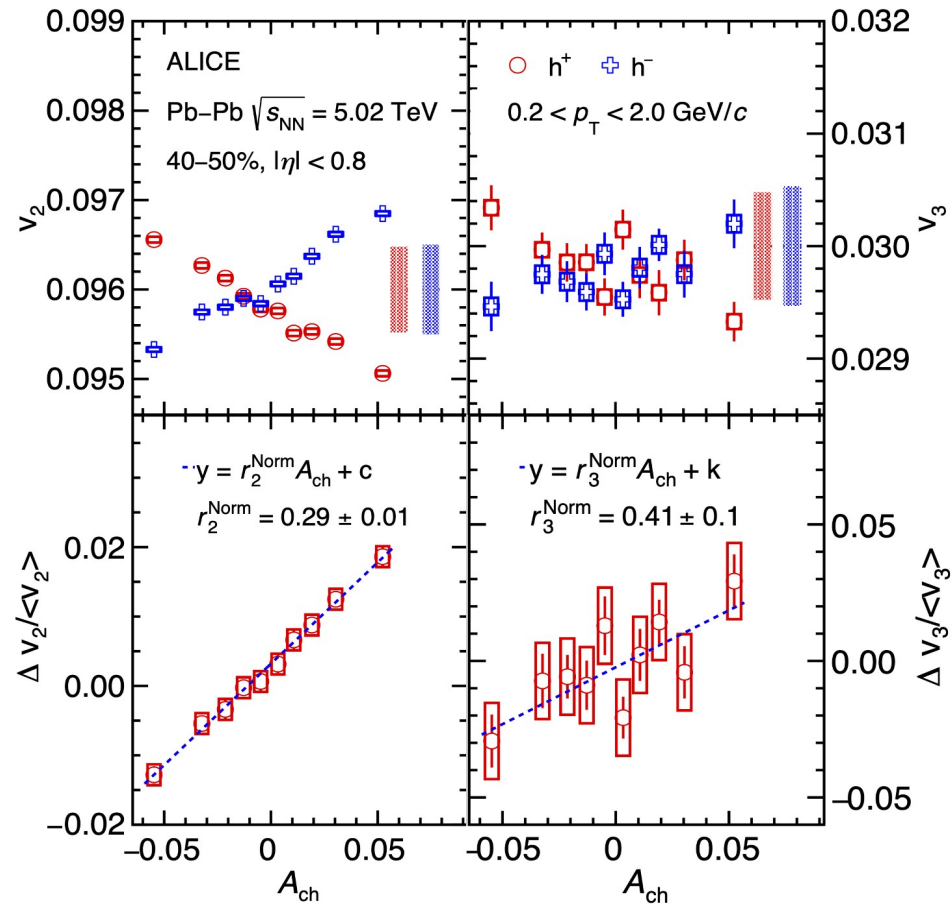
- Consistent with 0 for 0–30% and then becomes positive
- Combining the points from 0–70%
  - $f_{\text{CME}}^{\text{Xe}} = -0.003 \pm 0.010 \rightarrow 2\% \text{ at 95\% C.L.}$
  - $f_{\text{CME}}^{\text{Pb}} = 0.147 \pm 0.061 \rightarrow 25\% \text{ at 95\% C.L.}$

$$f_{\text{CME}} = \frac{sB}{sB + b v_2}$$

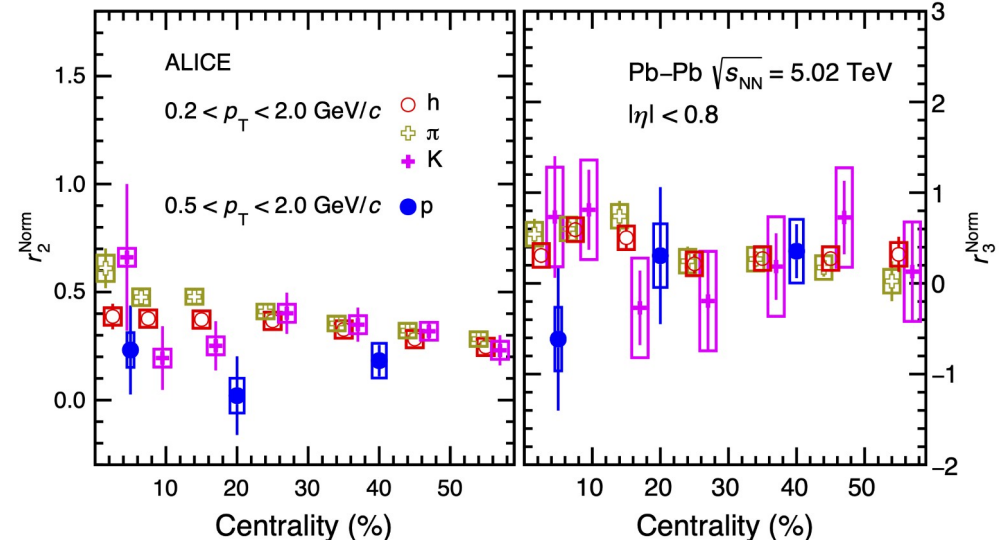
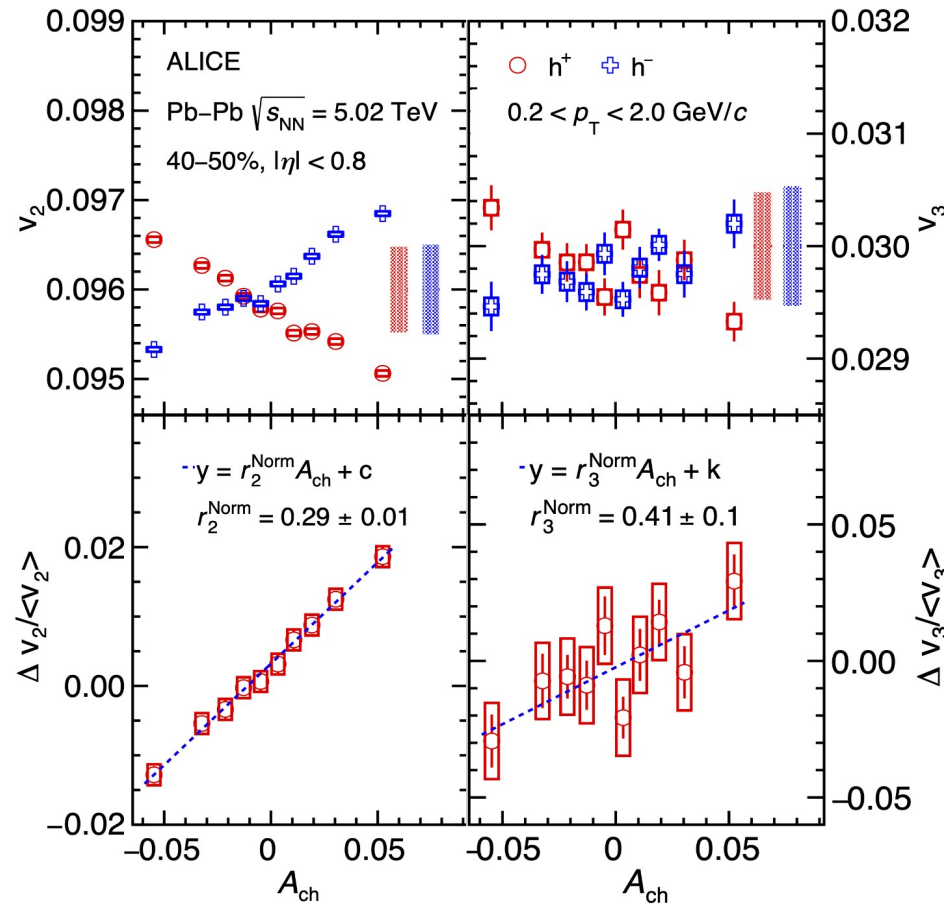


# Chiral Magnetic Wave

ALICE, JHEP 12, 067 (2023)

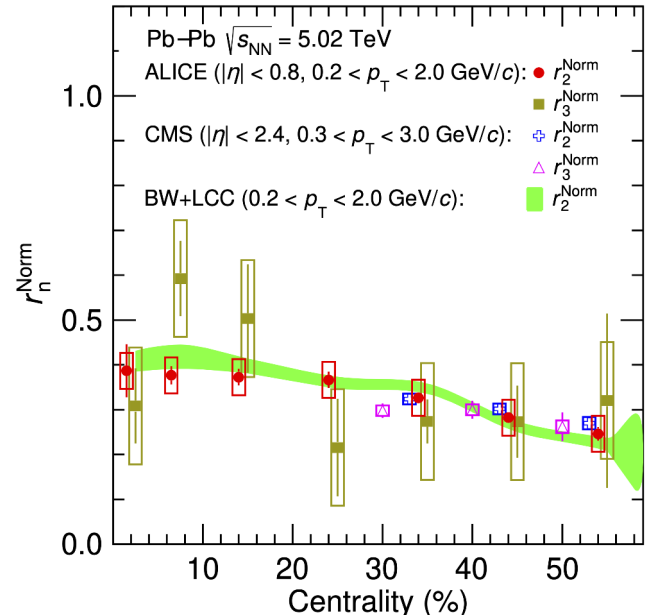
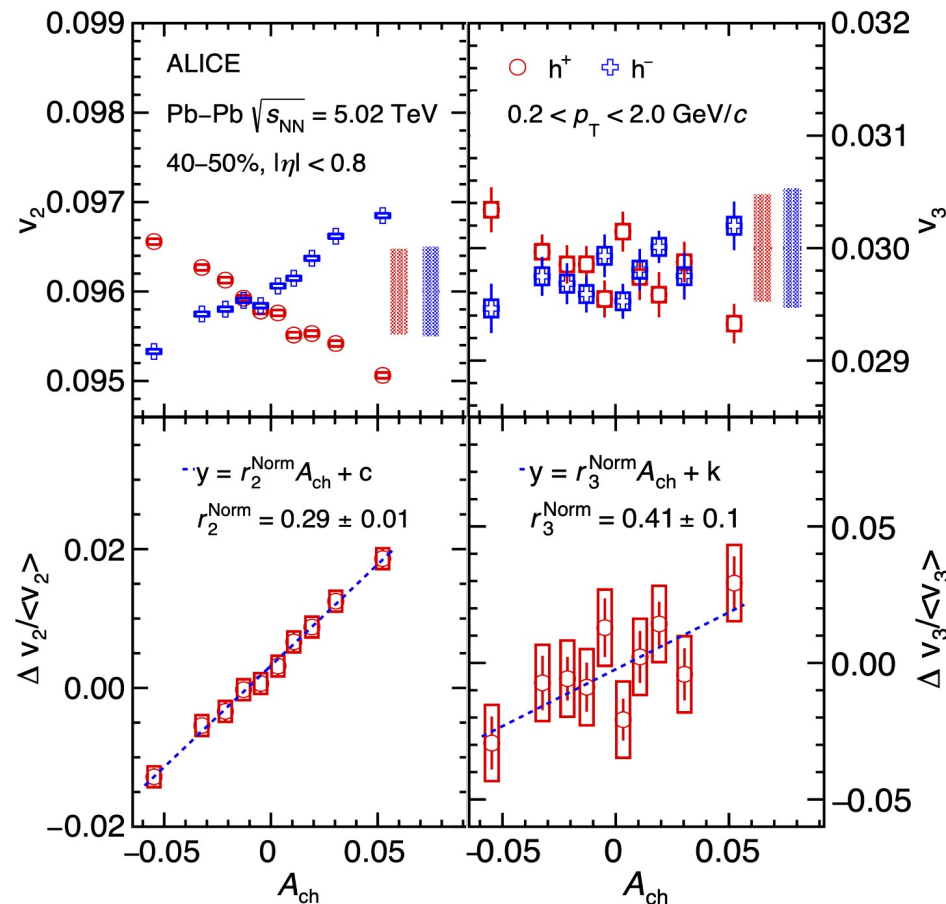
$v_2$  and  $v_3$  vs.  $A$ 

- Finite  $r_n^{\text{Norm}}$

$v_2$  and  $v_3$  vs.  $A$ 

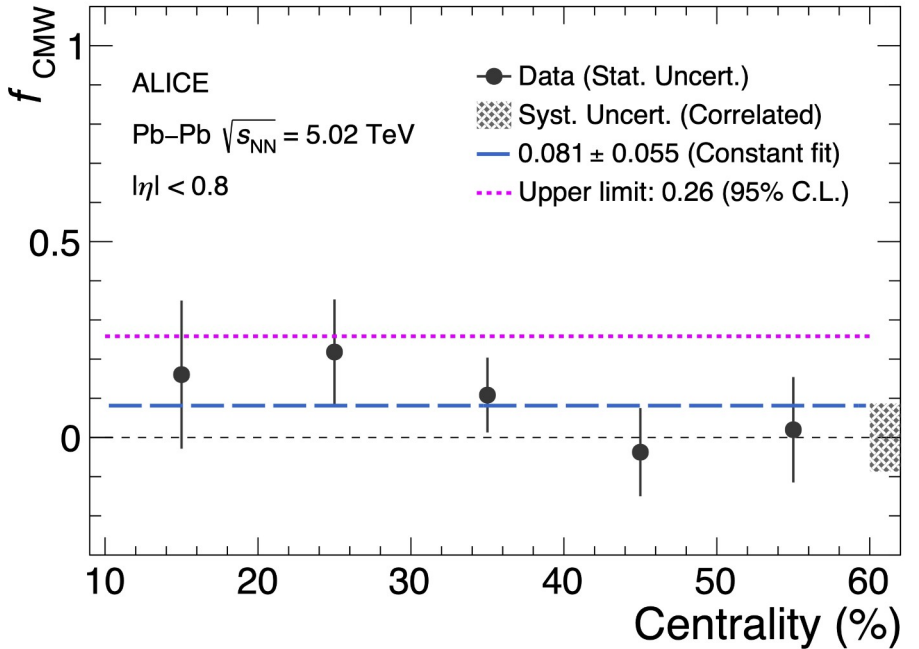
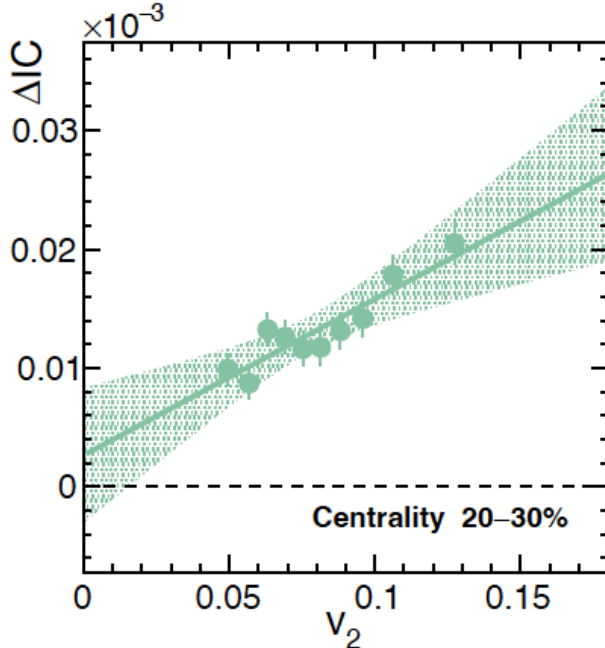
- Finite  $r_n^{\text{Norm}}$
- $r_2^{\text{Norm}}$  consistent with  $r_3^{\text{Norm}}$ 
  - No particle type dependence

# $v_2$ and $v_3$ vs. $A$



- Finite  $r_n^{\text{Norm}}$
- $r_2^{\text{Norm}}$  consistent with  $r_3^{\text{Norm}}$ 
  - No particle type dependence
- Good agreement with CMS results and BW calculations

# CMW fraction



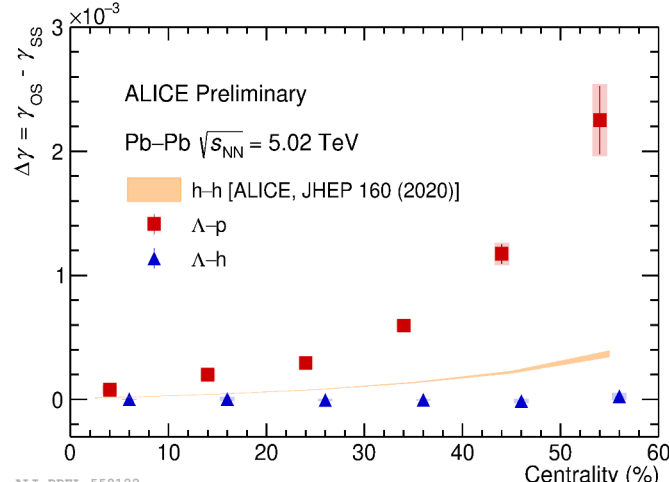
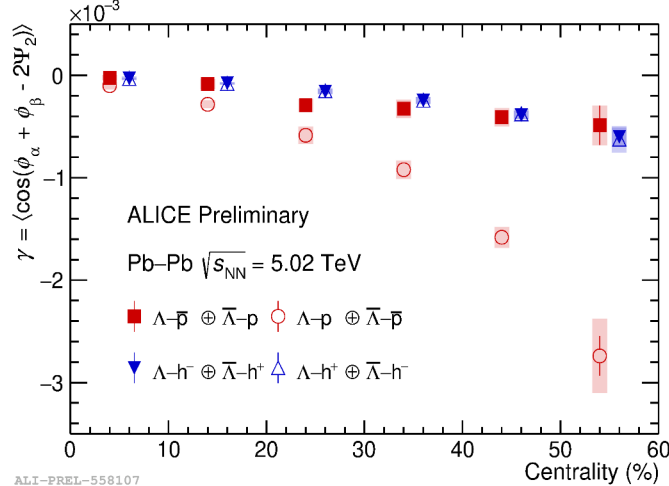
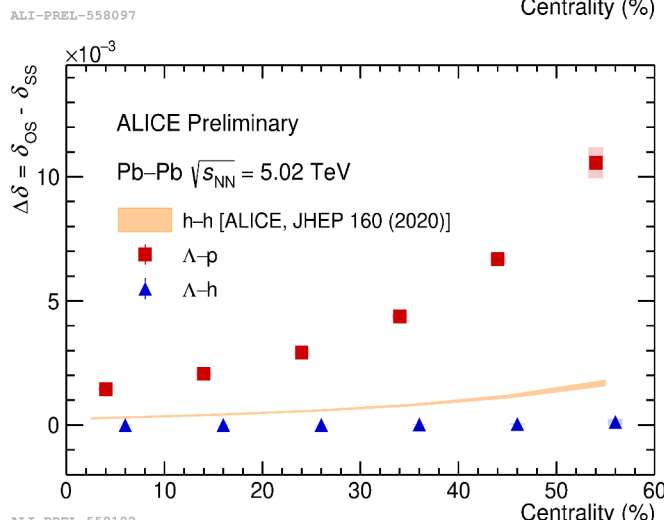
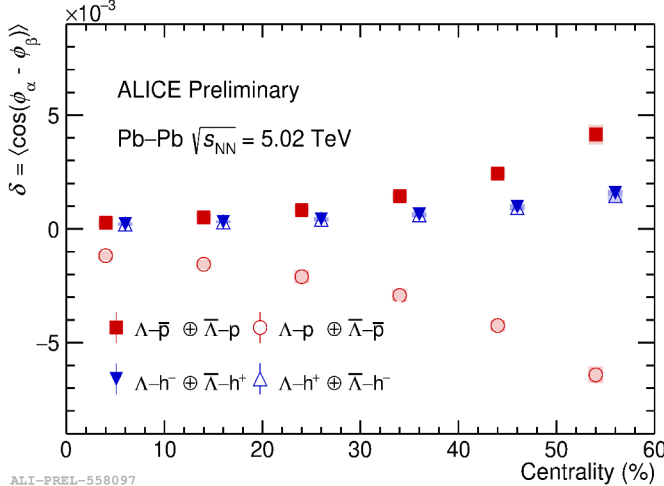
- $\Delta IC$  approximately scales with  $v_2 \rightarrow$  large background contribution
- $f_{CMW}$  extracted by fitting  $\Delta IC$  vs.  $v_2$  with a linear function  $av_2+b$
- Combining the points from 10–60 %
  - $f_{CMW} = 0.081 \pm 0.055 \rightarrow 26\%$  at 95% C.L.

$$f_{CMW} = \frac{b}{a \langle v_2 \rangle + b}$$

C. Wang et al., PLB 820, 136580 (2021)

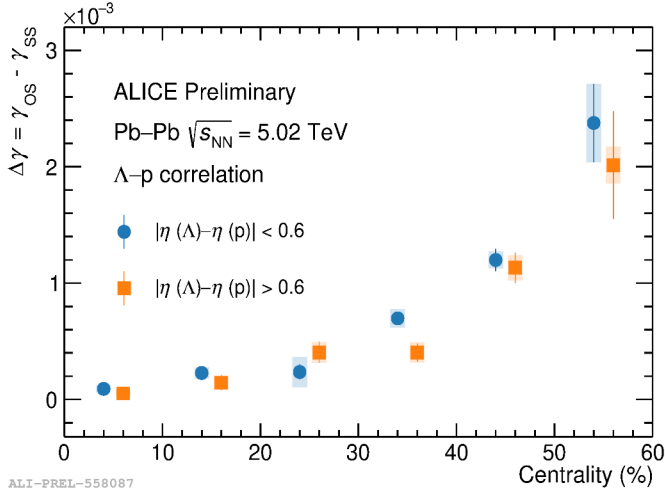
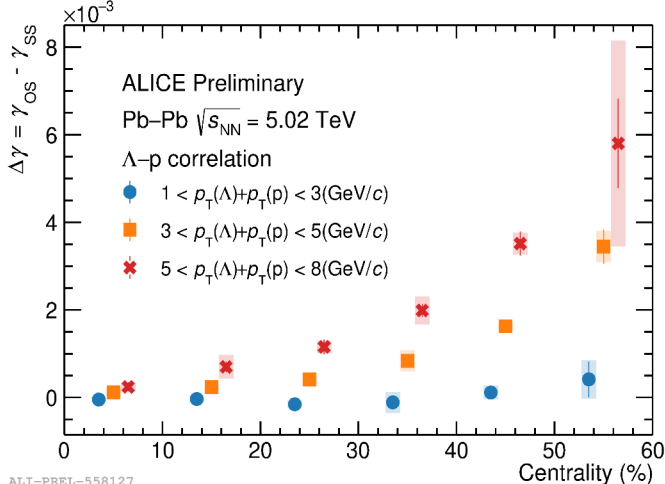
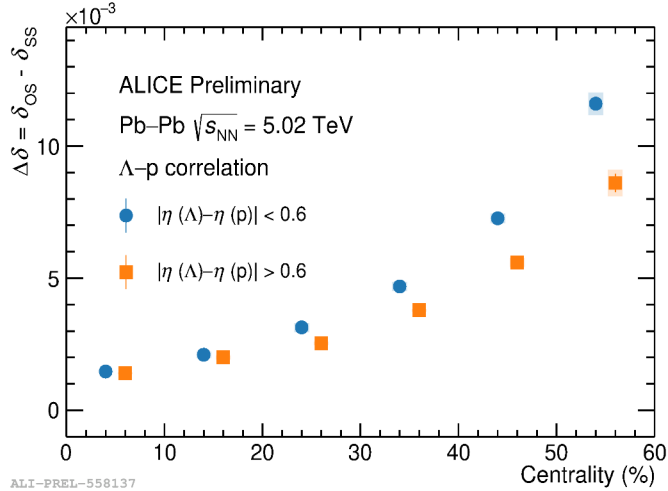
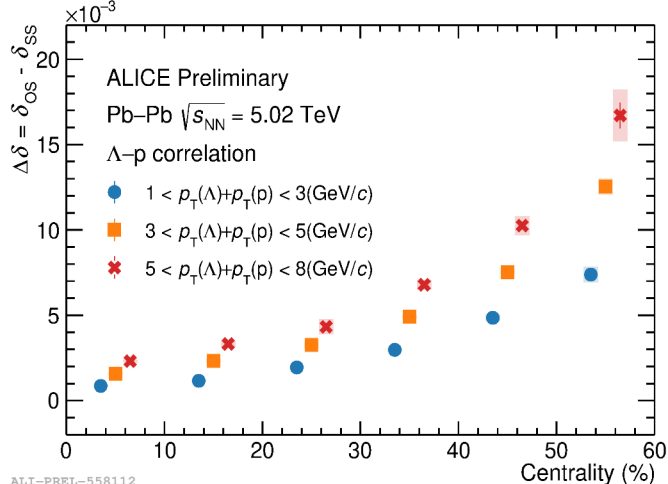
# Chiral Vortical Effect

## CVE



- Avoid CME ambiguity by using  $\Lambda$  baryon ( $\Lambda \rightarrow \pi p$ )
- Significant  $\delta$  and  $\gamma$  separation of  $\Lambda\text{-}p$ 
  - ~10 times larger than CME
  - Increasing with centrality
- Close to zero  $\delta$  and  $\gamma$  separation of  $\Lambda\text{-}h$

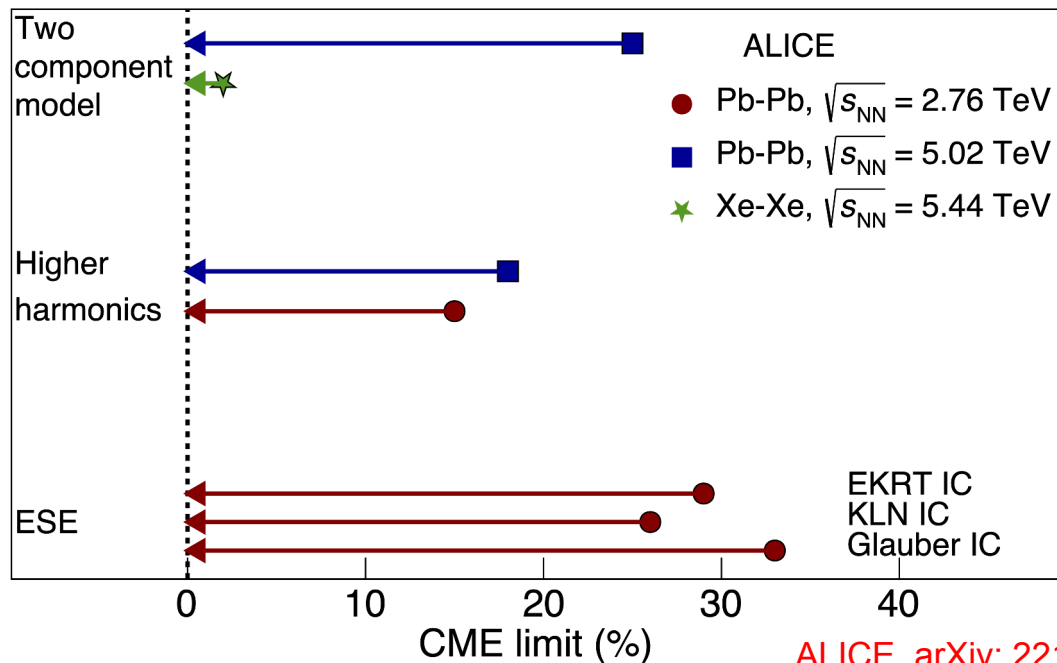
# CVE: differential analysis



- Larger  $\Delta\delta$  and  $\Delta\gamma$  for larger  $\sum p_T$
- Larger  $\eta$  gap  $\rightarrow$  small  $\Delta\delta$ 
  - Non-flow contributions?
- Larger  $\eta$  gap  $\rightarrow$  moderate  $\Delta\gamma$
- Constrain theoretical models

# Summary

- Anomalous chiral searches performed in different collision systems
  - Background dominates the measurements
  - Different approaches used to separate the signal from the background



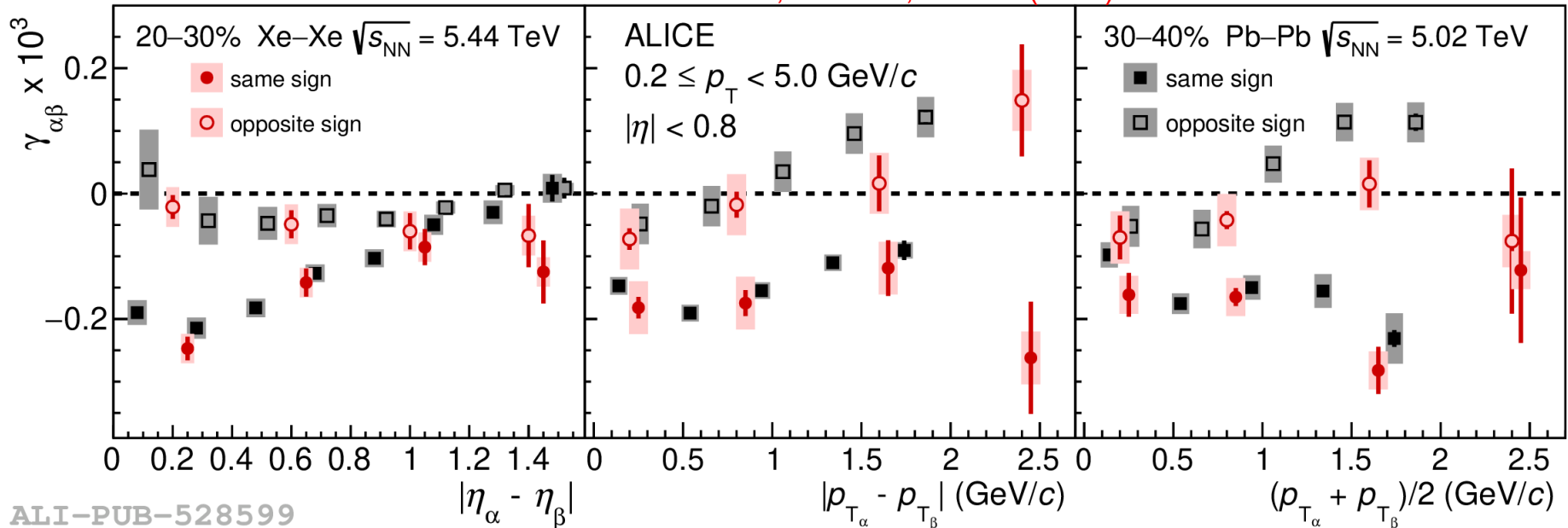


# Backup

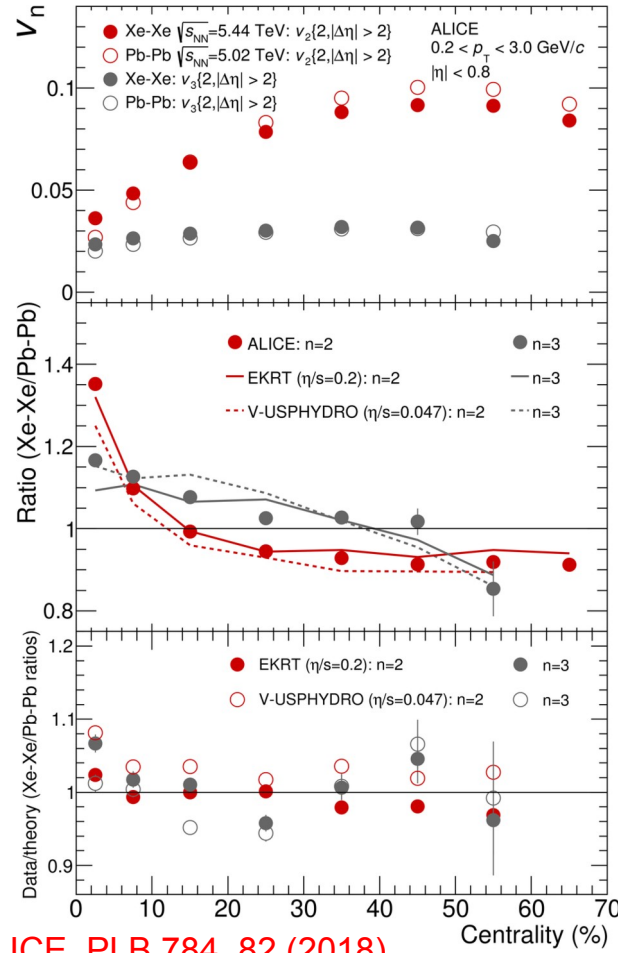


# 3-particle correlator: differential results in Xe–Xe and Pb–Pb collisions

ALICE, PLB 856, 138862 (2024)

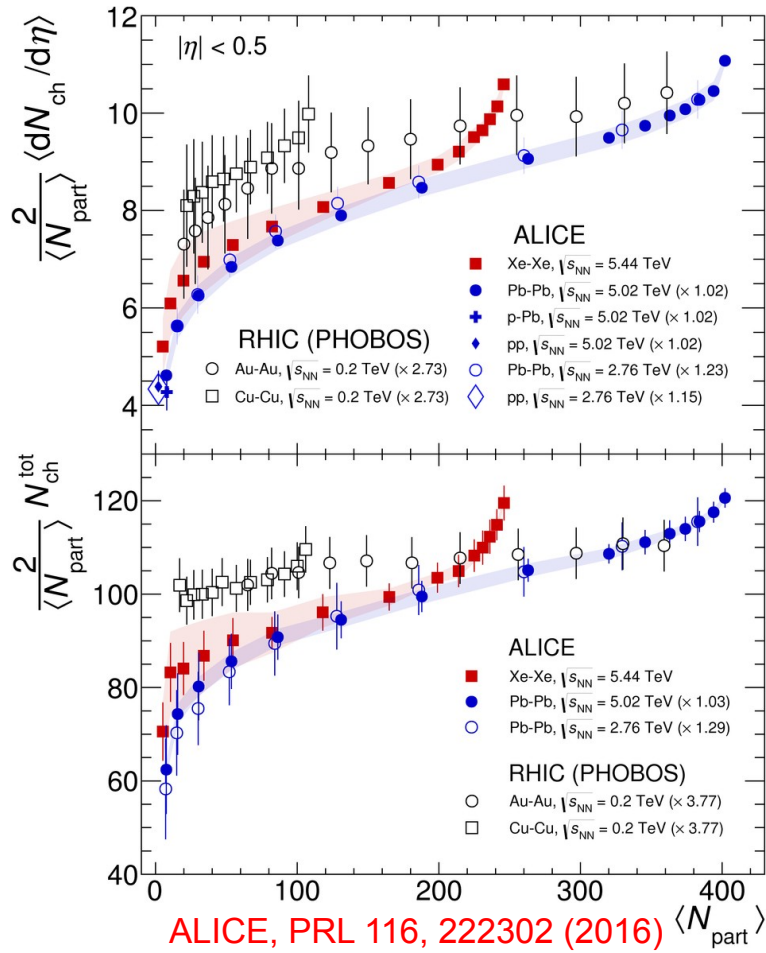


# $v_2$ and $dN_{\text{ch}}/d\eta$ in Xe–Xe and Pb–Pb collisions



ALICE, PLB 784, 82 (2018)

A. Dobrin - Chirality 2024



ALICE, PRL 116, 222302 (2016)

ALICE, PLB 790, 35 (2019)